ELECTROCHEMICAL CARBON DIOXIDE CAPTURE
TO CLOSE THE CARBON CYCLE

Supporting Information

Authors: R. Sharifian[1,2], R.M. Wagterveld[2], I. A. Digdaya[3], C. Xiang[3], D. A. Vermaas[1]

[1] Department of Chemical Engineering, Faculty of Applied Sciences, Delft University of Technology, The Netherlands.

[2] Wetsus, European Centre of Excellence for Sustainable Water Technology, Leeuwarden, The Netherlands.

[3] Division of Chemistry and Chemical Engineering, California Institute of Technology, Pasadena, California, USA.

This supporting information provides additional data, calculations, and correlations to the main text in three sections as described separately below.

1   Solubility of $CO_2(g)$ and carbonate minerals

The underlying correlations for obtaining Figure 4.a and b of the main paper are given here. Subsequently, the values of the solubility product (i.e., K_{sp}) of the three main forms of calcium carbonate minerals and the effect of temperature and pH on K_{sp} are provided.

1.1   Solubility of $CO_2(g)$: Effect of the temperature, salinity, and pressure

The temperature (T, in K) dependent CO_2 solubility coefficient (K_0, in mol L atm^{-1}) and carbonic acid dissociation constants (K_1 and K_2) in water at 1 atm are given by:[1]

$$\log K_0 = 108.3865 + 0.01985076T - 6919.53/T - 40.45154 \log T + 669365/T^2$$

$$\log K_1 = -356.3094 - 0.06091964T + 21834.37/T + 126.8339 \log T - 1684915/T^2$$

$$\log K_2 = -107.8871 - 0.03252849T + 5151.79/T + 38.92561 \log T - 1684915/T^2$$

In seawater, K_0 depends on the salinity (S, in ‰) and temperature (T, in K), as expressed by:[2]

$$\ln K_0 = -58.0931 + 90.5069(100/T) + 22.2940 \ln(T/100) + S [0.027766 - 0.025888(T/100) + 0.0050578(T/100)^2]$$

The carbonic dissociation constants (K_1 and K_2) in seawater at 1 atm are represented by the following equations:[3]

$$\log K_1 = 43.6977 + 0.0129037S - 1.364 \times 10^{-4}S^2 - 2885.378/T - 7.045159 \ln T'$$

$$\log K_2 = 452.0940 - 13.142162S + 8.101 \times 10^{-4}S^2 - 21263.61/T - 68.483143 \ln T - (581.4428S + 0.259601S^2)/T - 1.967035S \ln T$$

where S is the salinity (in ‰). At an average seawater S = 34.8‰, the pressure dependent K_1

and K_2 of carbonic acid is given by:[4]

$$\log (K_1^P/ K_1^1) = 0.013 + 1.319 \times 10^{-3}\,P - 3.061 \times 10^{-6}\,PT - 0.161 \times 10^{-6}\,T^2 - 0.02 \times 10^{-6}\,P^2$$

$$\log (K_2^P/ K_2^1) = -0.015 + 0.839 \times 10^{-3}\,P - 1.908 \times 10^{-6}\,PT + 0.182 \times 10^{-6}\,T^2$$

where K_1^1 and K_2^1 are K_1 and K_2 at 1 atm, and K_1^P and K_2^P at P atm. These equations are valid for temperature range between 2 °C and 22 °C and pressures up to 1000 atm.

1.2   Solubility of carbonate minerals: Effect of the temperature and pH

Uptake and release of carbon at alkaline pH usually involve precipitation of carbonate mineral through the reaction of CO_3^{2-} with divalent cation such as Ca^{2+} (i.e., $CaCO_3$). The solubility of $CaCO_3$ depends on the pH due to the hydrolysis of CO_3^{2-}. At 25 °C and 1 atm the Solubility product (K_{sp}) is 3.31×10^{-9} for calcite, 4.61×10^{-9} for aragonite, and 1.22×10^{-8} for vaterite. Figure S.1a and b below show the K_{sp} of various $CaCO_3$ crystal forms at temperature range between 0 and 90°C and the calcite solubility as a function of pH and temperature, respectively.
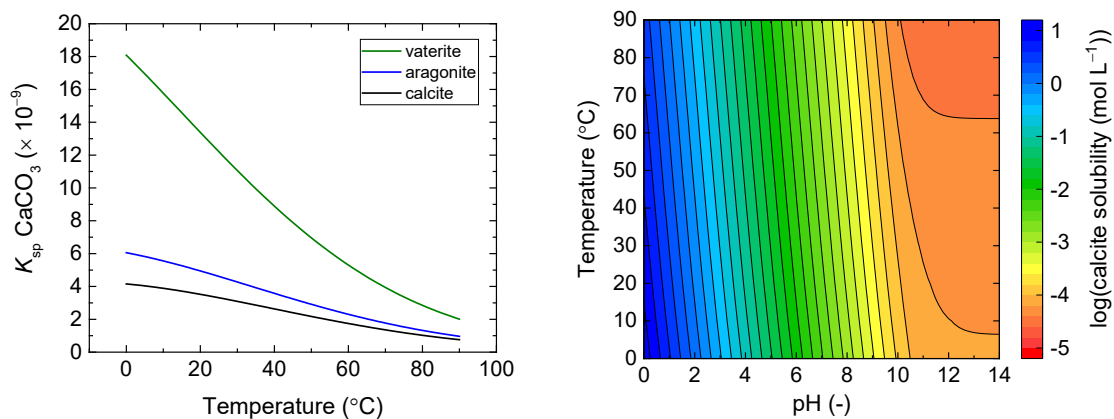

Fig. S.1 | (a) Solubility product (K_{sp}) of three different crystal forms of CaCO3 as a function of temperature. (b) Logarithmic calcite solubility in water as a function of the water pH and temperature.

The solubility products of calcite ($K_{sp,\ calcite}$), aragonite ($K_{sp,\ aragonite}$), and vaterite ($K_{sp,\ vaterite}$) at temperature range between 0 and 90 °C are given by:[1]

$$\log K_{sp,\ calcite}\quad = -171.9065 - 0.0077993T + 2839.319/T + 71.595 \log T$$

$$\log K_{sp,\ aragonite} = -171.9773 - 0.0077993T + 2903.293/T + 71.595 \log T$$

$$\log K_{sp,\ calcite}\quad = -172.1295 - 0.0077993T + 3074.688/T + 71.595 \log T$$

In seawater, at salinity range between 27 and 43‰ and temperature range between 2 and 25 °C, $K_{sp,\ calcite}$ is given by:[5]

$$K_{sp} = [-34.452 - 39.866 S^{1/3} + 110.21 \log S - 7.5752 \times 10^{-6}T^2] \times 10^{-7}$$

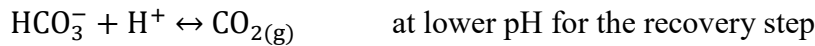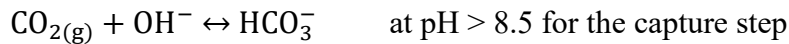The values of $K_{sp, calcite}$ as a function of pressure (P, in atm) in seawater is expressed by:[6]

$\ln (K_{sp, calcite}{}^{P}/K_{sp, calcite}{}^{1}) = 0.071320 + 0.0080412P - 2.2544 \times 10^{-5} \, PT$

where $K_{sp, calcite}{}^{1}$ is the solubility product of calcite at 1 atm and $K_{sp, calcite}{}^{P}$ is the solubility product of calcite at elevated pressure.

2   Electrical energy consumption for CO₂(g) capture: Electrolysis vs. BPMED

In this section, the underlying assumptions and calculations for obtaining Figure 14 of the main article body are provided. The aim here is to compare the electrical energy required for the $CO_{2(g)}$ capture and recovery using a pH-swing generated via (membrane) electrolysis and BPMED. As an example, the magnitude of pH swing here is considered to be $\Delta pH = 14$. The required voltage (hence the energy consumption) of both methods depends strongly on the magnitude of the applied ΔpH. Note that a milder ΔpH can enable lower energy consumptions.

Using both electrolysis and BPMED, 1 mole of OH^- and 1 mole of H^+ per mole of electron can be produced. Assuming the following reactions, each produced OH^- (or H^+) ion, contributes to 1 mole of CO₂(g) being captured (or recovered):

$CO_{2(g)} + OH^- \leftrightarrow HCO_3^-$ at pH > 8.5 for the capture step

$HCO_3^- + H^+ \leftrightarrow CO_{2(g)}$ at lower pH for the recovery step

According to the Faraday's law, the electric quantity (Q) to produce 1 mole CO₂(g) is 1 Faraday constant (F = 96485 C/mol). The energy involved in the pH swing can be calculate from eq. 11 from the main paper:

$$E = \frac{i \cdot A \cdot V}{r_{CO_2(g)}}$$

Assuming the Coulombic efficiency for the acid-base production is 100%, the energy consumption per mole of capture CO₂ (g) can then be calculated via $E = F \cdot V$

The required voltage for (membrane) electrolysis can be written as [7]:

$$V_{electrolysis} = E_{anode}^0 - E_{cathode}^0 + i \sum R = \underbrace{E_{cell}^0}_{\text{Standard cell potential}} + \underbrace{\eta_{H2/O2}}_{\text{Over-potential}} + \underbrace{i \sum R_{tot}}_{\text{Ohmic losses}}$$

Where E_{anode}^0 is the standard anode potential for oxygen evolution reaction (OER), $E_{cathode}^0$ is the standard cathode potential for hydrogen evolution reaction (HER), i is the applied current density, R_{tot} is the total ohmic resistivity and $\eta_{H2/O2}$ is the over potential at the anode and

3

cathode for OER and HER (i.e., the Tafel plot). The estimated value for each term is given in Table 1.S below.

Similarly, the required voltage for BPMED can be written as [8]–[10]:

$$V_{BPMED} = \underbrace{0.059\,\Delta pH}_{\text{Nernstian potential based on the reversible free enthalpy}} + \underbrace{\eta_{WDR}}_{\text{Over-potential}} + \underbrace{i\sum R_{tot}}_{\text{Ohmic losses}}$$

Where ΔpH is the difference of the pH over the BPM and η_{WDR} is the over potential associated with the water dissociation reaction in the junction layer of the BPM. The estimated value for each term is given in Table 2.S below.

For the calculations, electrochemical cells as shown in Figure S.2 are assumed. For BPMED, the effect of the end electrodes is neglected as multiple cell pair (CEM-AEM-BPM) can be stacked up in one unit, overruling the electrodes overpotential. In electrolysis stacking is not possible and the process is strongly dependent on the electrode reactions.
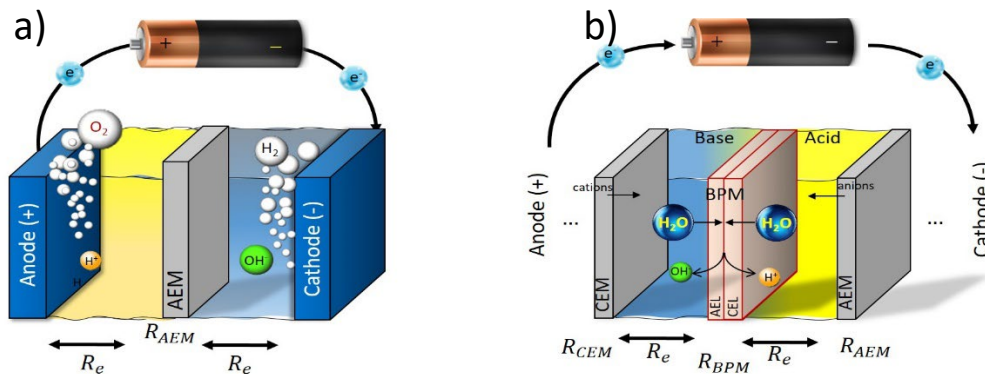

Figure S.2 | Schematic of the (membrane) electrolysis cell (a) and the BPMED cell (b) used for calculation of the electrical energy consumption of the electrochemical CO₂ (g) capture & recovery.

a) (Membrane) electrolysis: $E^0_{cell} + \eta_{H2/O2} + i\sum R_{tot}$

1. The standard cell potential, E^0_{cell} according for the water redox is as follow:

   - Cathode: $2H_2O + 2e^- \rightarrow H_{2(g)} + 2OH^-$ $E^0_{cathode} = -0.829\,V$ vs. SHE at pH=14
   - Anode: $2H_2O \rightarrow 4e^- + O_{2(g)} + 4H^+$ $E^0_{anode} = 1.23\,V$ vs. SHE at pH=0

   $E^0_{cell} = E^0_{anode} - E^0_{cathode} = 1.23 - (-0.829) = 2.059$ V for creating a ΔpH =14.

2. $\eta_{H2/O2}$ is approximately $2 \times 0.1 = 0.2$ V at current density i = 20 mA/cm² (based on the Tafel plot for HER and OER).

3. The ohmic voltage drop is $i\sum R_{tot}$, where $R_{tot} = R_e + R_m + R_b + R_c$ as shown in Table 1.S:

R_e (electrolyte resistance) for 0.5 M NaCl	$20 \ \Omega. cm^{2}$ [a]
R_m (membrane resistance)	$4 \ \Omega. cm^{2}$ [b]
R_c (circuit resistance)	neglected
$i \times R_b$ ($H_{2(g)}$ and $O_{2(g)}$ bubble ohmic losses)	0.2 V
Assuming i= 20 mA/cm²: $\quad$ **i ($R_e + R_m + R_b$) =**	**0.68 V**

[a] Assuming a 0.5M NaCl electrolyte: a conductivity of 47 mS/cm and a cell total thickness of 0.5×2 =1 cm so that $R_e = 20 \ \Omega. cm^2$. [b] Assuming an ion exchange membrane from Fumasep B.V. (FAB).

b) Ex-situ BPMED*: $0.059 \ \Delta pH + \eta_{WDR} + i \sum R_{tot}$*

Ex-situ here means that a neutral salt stream (e.g., NaCl) is used to produce high purity NaOH and HCl in BPMED. The produced acid and base are then used for $CO_2(g)$ capture and recovery in external gas absorption and desorption steps.

1. The reversible Nernstian voltage based on the free enthalpy for creating a ΔpH =14 over the BPM is $0.059 \times 14 = 0.826$ V [10].
2. η_{WDR}: reaction overpotential is estimated at 0.15 V [9].
3. $i \sum R$: The ohmic voltage losses can be estimated as shown in Table 2.S.

R_e (electrolyte resistance) for 0.5 M NaCl	$20 \ \Omega. cm^2$ [a]
$R_m : R_{CEM} + R_{BPM} + R_{AEM}$	4+10+4 =18 $\Omega. cm^2$ [b]
R_c (circuit resistance)	neglected
Assuming i= 20 mA/cm²: $\quad$ **i. ($R_e + R_m$) =**	**0.76 V**

[a] Assuming a 0.5M NaCl electrolyte: a conductivity of 47 mS/cm and a cell total thickness of 0.5×2 =1 cm so that $R_e = 20 \ \Omega. cm^2$. [b] assuming an IEM & BPM from Fumasep B.V.

3   The market size and price of CO₂ utilization products

Table S.3 below gives the values associated with Figure 17 of the main article body, showing the market size and price of CO₂ utilization products in various regions between 2018 and first quarter of 2020 (unless otherwise noted). CO₂ and H₂ market size and price are included for reference.

Table 3.S CO₂ utilization products market size and price

CO₂ utilization products	Market size (megatonne year^{-1})	Price ($ tonne^{-1})	Reference
Methane^a	2894	86 – 173	[11]–[13]
Ethane	120.27	139 – 180	[14]–[17]
Propane	195^b	317 – 374	[18]–[22]
Ethylene	184	474 – 609	[23]–[25]
Propylene	100	551 – 800	[26]–[29]
Methanol	98.9	174 – 235	[30]–[32]
Ethanol	86.8	45 – 1026	[33]–[36]
Isopropanol	2.15	750 – 3670	[37]–[39]
Acetone	6.1	906 – 1770^c	[40], [41]
Acetic acid	17.28	330^c	[42], [43]
Formic acid	1.02	225 – 332^c	[44], [45]
Urea	187.8	214 – 860	[46]–[49]
Carbon monoxide	150	236^d	[50]
Carbon dioxide	230	15 – 120	[51]
Hydrogen	102	1640 – 2500	[52]–[54]

^{a} assumes natural gas market size and price. ^{b} 2016 market size. ^{c} Chinese spot price. ^{d} 2014-2018 average price in United States.

References

[1]   L. N. Plummer and E. Busenberg, "The solubilities of calcite, aragonite and vaterite in CO2-H2O solutions between 0 and 90°C, and an evaluation of the aqueous model for the system CaCO3-CO2-H2O," *Geochim. Cosmochim. Acta*, vol. 46, no. 6, pp. 1011–1040, Jun. 1982.

[2]   R. F. Weiss, "Carbon dioxide in water and seawater: the solubility of a non-ideal gas," *Mar. Chem.*, vol. 2, no. 3, pp. 203–215, Nov. 1974.

[3]   F. J. Millero *et al.*, "Dissociation constants for carbonic acid determined from field measurements," *Deep Sea Res. Part I Oceanogr. Res. Pap.*, vol. 49, no. 10, pp. 1705–1723, Oct. 2002.

[4]   B. Acid, "OCEANOGRAPHY," vol. 1286, no. July, 1968.

[5]   S. E. Ingle, "Solubility of calcite in the ocean," *Mar. Chem.*, vol. 3, no. 4, pp. 301–319, Nov. 1975.

[6]   D. C. Plath, K. S. Johnson, and R. M. Pytkowicz, "The solubility of calcite — probably containing magnesium — in seawater," *Mar. Chem.*, vol. 10, no. 1, pp. 9–29, Oct. 1980.

[7]   M. Wang, Z. Wang, X. Gong, and Z. Guo, "The intensification technologies to water electrolysis for hydrogen production - A review," *Renew. Sustain. Energy Rev.*, vol. 29, pp. 573–588, 2014.

[8]   D. A. Vermaas, S. Wiegman, T. Nagaki, and W. A. Smith, "Ion transport mechanisms in bipolar membranes for (photo)electrochemical water splitting," *Sustain. Energy Fuels*, vol. 2, no. 9, pp. 2006–2015, 2018.

[9]   S. Z. Oener, M. J. Foster, and S. W. Boettcher, "Accelerating water dissociation in bipolar membranes and for electrocatalysis," *Science (80-.).*, p. eaaz1487, Jul. 2020.

[10]   H. Strathmann, H. J. Rapp, B. Bauer, and C. M. Bell, "Theoretical and practical aspects of preparing bipolar membranes," *Desalination*, vol. 90, no. 1–3, pp. 303–323, 1993.

[11]   "Natural gas production 2018," *International Energy Agency (IEA)*.

[12]   "Short-term energy outlook – Natural gas," *U.S. Energy Information Administration (EIA)*, 2020.

[13]   "Analysis: Low gas prices not enough for Asia to move away from coal," *S&P Global Platts*.

[14]   "Will the world have enough ethane?," *Strata Advisors*, 2018.

[15]   "US ethane price to rise in 2021 on declining availability, rising demand," *Chemical Week*, 2020.

[16]   "Mont Belvieu Ethane (OPIS) Average Price Option Quotes," *CME Group*, 2020.

[17]   "US petrochemical feedstock volatility could last through 2020: LyondellBasell CEO," *S&P Global Platts*, 2020.

[18]   "Propane Market Size Worth $106.9 Billion By 2025 | CAGR: 3.5%," *Grand View Research*, 2017.

[19]   "Petroleum & Other Liquids – Weekly Heating Oil and Propane Prices (October - March)," *U.S. Energy Information Administration (EIA)*, 2020.

[20]   "Asia faces costlier LPG as low US oil price prompts NGL estimate cuts," *S&P Global Platts*.

[21]   "Mont Belvieu LDH Propane (OPIS) Futures Quotes," *CME Group*.

[22]   "European Propane CIF ARA (Argus) Futures Quotes," *CME Group*.

[23]   "Rapid changes in the ethylene capacity world order," *Wood Mackenzie*, 2019.

[24]   "Mont Belvieu Ethylene (PCW) Financial Futures Quotes," *CME Group*.

[25]   "European ethylene oversupply intensifies amid lockdowns, price at 11-year low," *S&P Global Platts*, 2020.

[26]   "Propylene Global Supply Demand Analytics Service," *Wood Mackenzie*, 2018.

[27]   "US propylene contracts see first price increase in nine months: sources," *S&P Global Platts*, 2020.

[28]   "European propylene prices move higher, supported by stronger feedstocks," *S&P Global Platts*, 2020.

[29]   "Asia-Pacific propylene prices fall from 11-week high," *Argus*, 2020.

[30]   "The methanol industry," *Methanol Institute*. .

[31]   "Platts Asia Methanol Assessments," *S&P Global Platts*, 2020.

[32]   "Methanol price and supply/demand," *Methanol Institute*.

[33]   "Annual fuel ethanol production – U.S. and world ethanol production," *RFA*.

[34]   "T2 ethanol price at pre-coronavirus levels on strong demand, tight undenatured supply," *S&P Global Platts*, 2020.

[35]   "US ethanol crush margin rebounds on higher prices, lower corn," *S&P Global Platts*,

2020

[36] "Ethanol market and pricing data – August 25, 2020," *U.S. Grains Council*, 2020.

[37] "Global Isopropyl Alcohol Market to Reach a Volume of 2.48 Million Tons by 2025," *Expert Market Research*.

[38] "European IPA at record high as production of sanitary products ramps up," *S&P Global Platts*, 2020.

[39] Y. Koh, "Southeast Asia IPA prices hit six-year high, market warns of peak," *Independent Commodity Inteligence Services (ICIS)*, 2020.

[40] "An incisive, in-depth analysis on the acetone market," *Future Market Insights*, 2016.

[41] "China's acetone prices triple on import duties, demand," *Argus*, 2020.

[42] "Global Acetic Acid Market to Reach 24.51 Million Tons by 2025," *Expert Market Research*.

[43] "China CN: Market Price: Monthly Avg: Organic Chemical Material: Acetic Acid," *CEIC*, 2020.

[44] "Worldwide Formic Acid Market Size to Reach USD 119.86 Million by 2026," *Market Watch*, 2020.

[45] "China CN: Market Price: Monthly Avg: Organic Chemical Material: Formic acid 94%," *CEIC*, 2020.

[46] "Global Urea Market: By Application: Fertilizer, Urea Formaldehyde (UF) & Melamine Resins, Melamine (Cyanurates), Animal Feed; By Region: North America, Europe, Asia Pacific, Latin America, Middle East & Africa; Historical Production and Consumption (2015-," *Expert Market Research*.

[47] "DTN Fertilizer Trends – Urea, Anhydrous Lead Retail Fertilizer Prices Lower," *DTN*, 2020.

[48] "World Bank Commodities Price Data (The Pink Sheet)," *World Bank*, 2020.

[49] "China's prilled urea sellers await return of India," *Argus*, 2020.

[50] R. G. Grim, Z. Huang, M. T. Guarnieri, J. R. Ferrell, L. Tao, and J. A. Schaidle, "Transforming the carbon economy: challenges and opportunities in the convergence of low-cost electricity and reductive CO_2 utilization," *Energy Environ. Sci.*, vol. 13, no. 2, pp. 472–494, 2020.

[51] "Putting CO2 to use – Creating value from emissions," *International Energy Agency (IEA)*, no. September, p. 86, 2019.

[52] E. Connelly, A. Elgowainy, and M. Ruth, "DOE Hydrogen and Fuel Cells Program Record," 2019.

[53] "Path to hydrogen competitiveness – A cost perspective," *Hydrogen Council*, 2020. .

[54] "The future of hydrogen – Seizing today's opportunities," *International Energy Agency (IEA)*, p. Accessed: August 2020, 2020.